Ternary CdSxSe1-x deposited on Ag(111) by ECALE: synthesis and characterization

Ternary CdS_xSe_{1-x} Deposited on Ag(111) by ECALE: Synthesis and Characterization

M. L. Foresti,*,† S. Milani,† F. Loglio,† M. Innocenti,† G. Pezzatini,† and S. Cattarin‡

Dipartimento di Chimica, Università di Firenze, Via della Lastruccia 3, 50019 Sesto Fiorentino (FI), Italy, and Istituto per l'Energetica e le Interfasi del CNR, Corso Stati Uniti 4, 35127 Padova, Italy

Received January 21, 2005. In Final Form: April 22, 2005

Morphology and electronic properties of CdS, CdSe, and the ternary compounds of formula CdS_xSe_{1-x} deposited on Ag(111) by ECALE have been characterized as a function of the composition. The number of the attainable x values is limited by the necessity of using well-defined CdS/CdSe deposition sequences. However, the quantitative analysis carried out by XPS and electrochemical stripping experiments indicates that the ECALE method has a good control on composition. The AFM images together with the electrochemical characterization indicate both two-dimensional and three-dimensional growth contributions. The photospectra recorded at CdS film electrodes in liquid junction with an alkaline (poly)sulfide electrolyte show good efficiency of photoconversion and band gap typical of the single crystal. Lower photoconversion efficiency and the presence of subband gap response are observed for CdSe; a possible reason is some crystalline disorder due to lower control of the layer-by-layer deposition in the case of Se. The dependence of band gap on composition of ternary CdS_xSe_{1-x} ECALE films is monotonic and in agreement with literature data reported for bulk materials.

Introduction

The interest in the electrochemical deposition of group II−VI compounds, in particular cadmium chalcogenides, stems from its ability to produce good quality materials with a relatively simple, soft procedure, operating at low temperature. Literature reports include preparation of layers of different thickness on various substrates, for potential applications going from solar energy conversion[1−3] to optoelectronics.[4,5] Recently, the electrochemical atomic layer epitaxy (ECALE) method has been proposed by Stickney and co-workers[6,7] for the deposition of well ordered group II−VI compounds. In the ECALE procedure, a binary compound is obtained by alternating the layer-by-layer underpotential deposition of the metallic and nonmetallic elements.[6,7] The approach, initially developed for polycrystalline as well as for single-crystal gold substrates, was extended by our group to Ag(111) substrate.[8,9] One major advantage of ECALE method consists of the possibility of optimizing separately the different steps of the alternate electrodeposition by adjusting the solution and potential parameters.

The deposition of ternary group II−VI compounds offers the possibility of tuning the band gap to meet specific needs, but poses the challenge of control on film composition. In our laboratory, experience in the ECALE growth of ternary group II−VI compound semiconductors was obtained by depositing $Cd_xZn_{1-x}S$ and $Cd_xZn_{1-x}Se$ on Ag (111).[10] The ternary chalcogenide $Cd_xZn_{1-x}S$ was obtained by a procedure corresponding to the alternate deposition of CdS and ZnS in submonolayer amounts; the compound stoichiometry depends on the ZnS/CdS deposition sequence in a well-defined and reproducible way, with the limit that only certain discrete x values are attainable, depending on the adopted ZnS/CdS deposition sequence. Then, photoelectrochemical measurements confirmed that the band gap values of $Cd_xZn_{1-x}S$ vary about linearly with composition parameter x between 2.42 eV of CdS and 3.66 eV of ZnS,[11] a dependence consistent with the formation of solid solutions in a system without miscibility gap and one close to the literature relation established for bulk materials.[12]

Concerning ternary compounds like cadmium sulfoselenides CdS_xSe_{1-x}, thin film preparation by different techniques has been reported in the literature: vacuum evaporation,[13] spray pyrolysis,[14] electrochemical deposition,[15,16] and chemical bath deposition.[17] Epitaxial CdS_xSe_{1-x} layers, although limited to compounds with less than 12% selenium, were grown on InP(111)[18] and on

* Corresponding author. Telephone: +390554573107. Fax +390554573385. E-mail: foresti@unifi.it.

† Università di Firenze.

‡ Istituto per l'Energetica e le Interfasi del CNR.

(1) Miller, B.; Heller, A. *Nature (London)* **1976**, *262*, 680.

(2) Danaher, W. J.; Lyons, L. E. *Nature (London)* **1978**, *271*, 139.

(3) Panicker, M. P. R.; Knaster, M.; Kroger, F. A. *J. Electrochem. Soc.* **1978**, *125*, 566.

(4) Lincot, D.; Kampmann, A.; Mokili, B.; Vedel, J.; Cortes, R.; Froment, M. *Appl. Phys.* Lett. **1995**, *67*, 2355.

(5) Cachet, H.; Cortes, R.; Froment, M.; Maurin, G. *J. Solid-State Electrochem.* **1997**, *1*, 100.

(6) Gregory, B. W.; Stickney, J. L. *J. Electroanal. Chem.* **1991**, *300*, 543.

(7) Colletti, L. P.; Flowers, B. H. Jr.; and Stickney, J. L. *J. Electrochem. Soc.* **1998**, *145*, 1442.

(8) Pezzatini, G.; Caporali, S.; Innocenti, M.; Foresti, M. L. *J. Electroanal. Chem.* **1999**, *475*, 164−170.

(9) Innocenti, M.; Pezzatini, G.; Forni, F.; Foresti, M. L. *J. Electrochem. Soc.* **2001**, *148*, C357−C362.

(10) Loglio, F.; Innocenti, M.; Pezzatini, G.; Foresti, M. L. *J. Electroanal. Chem.* **2004**, *562*, 117−125.

(11) Innocenti, M.; Cattarin, S.; Loglio, F.; Cecconi, T.; Seravalli, G.; Foresti, M. L. *Electrochim. Acta* **2004**, *49*, 1327−1337.

(12) Landolt-Börnstein, In *Numerical Data and Functional Relationships in Science and* Technology; Madelung, O., Ed; Springer-Verlag: Berlin 1982; Vol. 17b.

(13) Noufi, R. N.; Kohl, P. A.; Bard, A. J. *J. Electrochem. Soc.* **1978**, *125*, 375.

(14) Feigelson, R. S.; N'Diaye, A.; Yin, S.-Y.; Bube, R. H. *J. Appl. Phys.* **1977**, *48*, 3162.

(15) Loufty, R. O.; Ng, D. S. *Solar Energy Mat.* **1984**, *11*, 319−328.

(16) Premaaratne, K.; Akuranthilaka, S. N.; Dharmadasa, I. M.; Samantilleka, A. P. *Renewable Energy* **2003**, *29*, 549−557.

(17) Mane, R. S.; Lokhande, C. D. *Thin Solid Films* **1997**, *304*, 56−60.

(18) Claybourn, M.; Scott, M. D.; Williams, J. O.; Goodfellow, R. C. *J. Cryst. Growth* **1982**, *58*, 417−424.

10.1021/la050176k CCC: $30.25
Published on Web 06/09/2005

GaAs(111)[19] by hot wall beam epitaxy. This paper reports on the electrodeposition of CdS_xSe_{1-x} on Ag(111) by ECALE, which is made possible by the compatibility of the deposition processes of S and Se.[8] The characterization includes the following: AFM investigations of morphology; evaluation of composition by XPS and stripping analysis; photoelectrochemical investigations of electronic properties.

Experimental Section

ECALE Film Deposition. Fluka analytical reagent grade $Na_2SeO_3 \cdot 5H_2O$, Merck analytical reagent grade $3CdSO_4 \cdot 8H_2O$, $HClO_4$, NH_4OH, $CH_3COONa \cdot 3H_2O$, CH_3COOH, and Aldrich analytical reagent grade Na_2S were used without further purification. $HClO_4$ and NH_4OH were used to prepare the pH 9.6 ammonia buffer, whereas $CH_3COONa \cdot 3H_2O$ and CH_3COOH were used to prepare the pH 5 acetic buffer. The solutions were freshly prepared just before the beginning of each series of measurements. An automated deposition apparatus, consisting of Pyrex solution reservoirs, solenoid valves, a distribution valve, and a flow-cell, was used under the control of a computer. Both the distribution valve and the cell were designed and realized in the workshop of our department.[9] The working electrodes were silver single crystals grown by the Bridgman technique and cut as to form disks with about 1 cm in diameter.[20] Before their use in the electrochemical cell, the working electrodes were chemically polished with solutions of 0.15 M CrO_3 in 0.1 M HCl. After polishing, the electrode was soaked first in concentrated ammonia for about 5 min, and then in concentrated sulfuric acid for about 20 min. Finally, it was rinsed thoroughly with water.[21] The counter electrode was gold foil, and the reference electrode was an Ag/AgCl/saturated KCl placed on the outlet tubing of the cell.

Composition Measurements. The composition of samples was estimated by X-ray photoelectron spectroscopy (XPS). The measurements were performed in a vacuum system capable of base pressure in the low 10^{-9} Torr range, equipped with a multichannel hemispherical electron analyzer using Mg Kα sources.

AFM Measurements. Topography was measured ex situ in a dry nitrogen atmosphere, using a Molecular Imaging AFM (PicoSPM, Molecular Imaging) operating in contact mode, with a commercial Si_3N_4 cantilever (Nanosensors, Wetzlar-Blankenfeld). The samples were characterized by nonfiltered 512×512 pixels images of areas ranging from 5×5 to 10×10 μm^2.

Photoelectrochemical Characterization. Photoelectrochemical experiments were performed with electrodes prepared by fixing the silver substrate with conducting silver epoxy to a brass rod and sealing with epoxy resin; only the area covered by the thin semiconductor film was exposed to the electrolyte. Investigations were performed either in 1 M NaOH, in 1 M Na_2S, in 50 mM S, or in the corresponding sulfur free solution, which is transparent until the lower explored limit of 400 nm. Solutions were prepared from water deionized by a Millipore Milli-RO system and analytical grade reagents purchased from Carlo Erba and Merck, used without further purification.

The Pyrex electrochemical cell, with a three-electrode configuration, was equipped with a quartz optical flat on the side. A saturated calomel electrode (SCE) was used as reference and all potentials are given vs SCE. To limit (photo)oxidation processes, during experiments the cell was maintained under a nitrogen stream. A standard photoelectrochemical set up was used: 150 W Xe lamp; monochromator (Applied Photophysics); filters (Schott); light chopper (EG&G Brookdeal model 9479); potentiostat and function generator (Amel models 553 and 568, respectively); lock-in amplifier (PAR model 5210). Monochromatic light power was measured with a calibrated photodiode (Macam Photometrics). Photocurrent spectra were measured under a chopped light (chopping frequency 3−4 Hz).

Results and Discussion

Preliminary Investigation of Se Deposition on Ag(111). The attainment of Se_{UPD} layers on Ag(111) is quite different from that of S_{UPD} layers. The latter are simply obtained from sulfide ions solutions by applying a potential slightly less positive than that required for bulk oxidation of sulfide ions. On the contrary, the chemical instability of selenide ions solutions prevents the direct underpotential oxidation.

Therefore, the formation of the first layer of Se on Ag(111) is obtained by a two-step procedure very similar to that adopted on gold:[22,23] briefly, an excess of Se(0) is deposited, and then the potential is fixed at values sufficient to reduce bulk selenium, but not the Se layer, which is most strongly bound to the surface and which must, therefore, be considered the UPD layer.[8] As reported in the literature[24,25] the Se(0) obtained by the direct reduction of Se(IV) solutions is electroinactive ("gray" selenium) and tends to passivate the electrode. On the contrary, the only electroactive form of Se(0) is "red" selenium, which is obtained by the chemical conproportionation reaction:[26,27]

$$H_2SeO_3 + 2H_2Se \rightarrow 3Se + H_2O \qquad (1)$$

This behavior has been confirmed in a detailed investigation of Se(IV) electrochemistry on silver that has been recently carried out in our laboratory.[28] A small part of Se(−II) is formed by the direct reduction of Se(IV) in a reaction path involving six electrons, which is almost parallel to the reaction path giving "gray" Se(0). Having been formed in a Se(IV) solution, this even small part of Se(−II) produces "red" Se(0). Then, when applying a potential sufficiently negative to reduce Se(0), more Se(−II) is formed, that again reacts with Se(IV) to give more "red" Se(0). Briefly, a regime of two competitive processes is established: the first one leading to the formation of "red" Se(0), and the second one leading to its reduction.

Figure 1a shows the progressive evolution of cyclic voltammograms of Se(IV) as obtained by a continuous scan from −0.4 to −1.15 V in a pH 8.5 ammonia buffer solution. The large peak preceding hydrogen evolution corresponds to the reduction of the chemically formed Se(0) to Se(−II). This peak does not appear in the first scan, when the amount of red Se(0) is still low. However, it appears in the second scan and rapidly reaches a limiting value, thus indicating steady-state conditions. As suggested by eq 1, the peak height depends on Se(IV) concentration. In light of the above behavior, the application of a potential sufficiently negative surely involves "red" Se(0) formation. The UPD layer of Se is then obtained by further reducing the excess of Se(0). However, the reduction must be performed in the absence of Se(IV) to avoid the conproportionation reaction 1. Thus, after depositing Se(0), the Na_2SeO_3 solution must be replaced by a solution of the supporting electrolyte alone.

(19) Grün, M.; Gerlach, H.; Breitkopf, Th.; Hetterich, M.; Reznitskyy, A.; Kalt, H.; Klingshirn, C. *J. Cryst. Growth* **1995**, *146*, 414−417.
(20) Hamelin, A. In *Modern Aspects of Electrochemistry*; Conway, B. E., White, R. E., Bockris, J. O'M., Eds.; Plenum Press: New York, 1985; Vol. 16, p 1.
(21) Hamelin, A.; Stoicoviciu, L.; Doubova, L.; Trasatti, S. *J. Electroanal. Chem.* **1988**, *244*, 133.
(22) Villegas, I.; Napolitano, P. *J. Electrochem. Soc.* **1999**, *146*, 117.
(23) Wade, T. W.; Flowers, B. H.; Vaidyanathan, R.; Mathe, K.; Maddox, B.; Happek, U.; Stickney, J. *Proceedings of the 197th Meeting of the Electrochemical Society; Toronto, 14−18 May, 2000*; The Electrochemical Society: Pennington, NJ, 2000.
(24) Liu, D.; Zhang, Y.; Zhou, S. *J. Xiamen Univ.* **1989**, *28*, 495.
(25) Wei, C.; Myung, N.; Rajeshwar, K. *J. Electroanal. Chem.* **1994**, *375*, 109.
(26) Tomkiewicz, M.; Ling, I.; Parsons, W. S. *J. Electrochem. Soc.* **1982**, *129*, 2016.
(27) Vazquez, M. D.; Batanero, P. S. *Electrochim. Acta* **1992**, *37*, 1165.
(28) Pezzatini, G.; Loglio, F.; Innocenti, M.; Foresti, M. L. *Collect. Czeck. Chem. Commun.* **2003**, *68*, 1579.

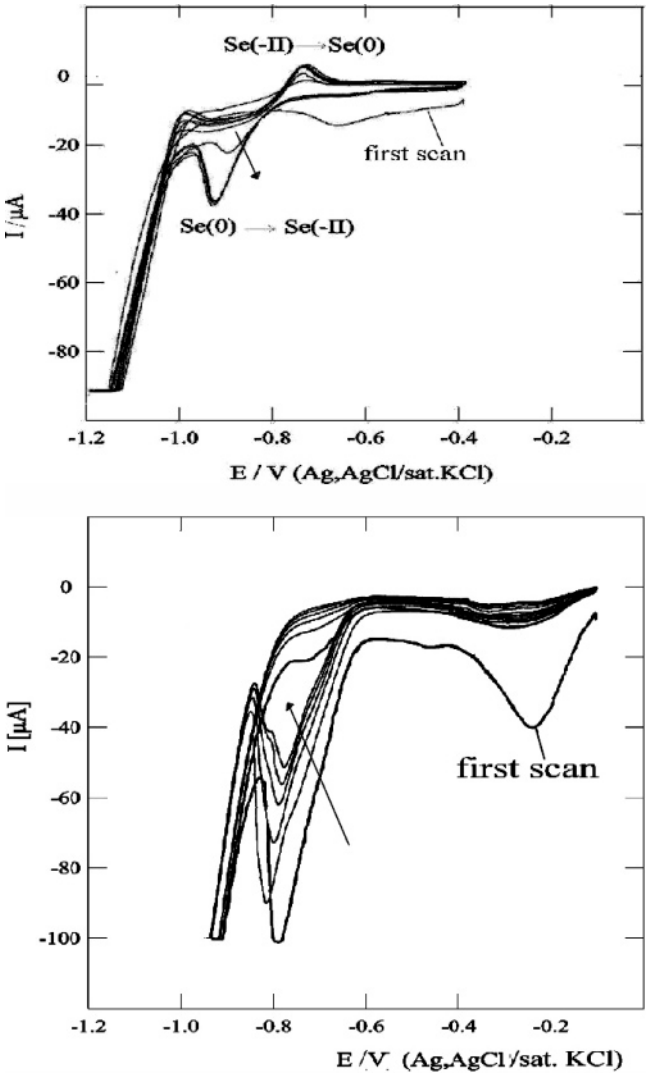

Figure 1. Consecutive CVs of 8×10^{-4} M Se(IV) solutions recorded from −0.4 to −1.2 V/Ag,AgCl in pH 8.5 ammonia buffer (a) and from −0.1 to −0.9 V/Ag,AgCl in pH 5 acetic buffer (b) on Ag(111). The arrows indicate the evolution of the curves. The scan rate was 50 mV s^{-1}.

Despite the two-step procedure, the experimental conditions for the attainment of Se_{UPD} on Ag(111) are not critical. In fact, the optimum potential for Se deposition from pH 8.5 ammonia buffer solutions ranged from −0.86 to −0.9 V.[29] However, as pointed out by preliminary experiments, this potential range is negative enough to cause partial S reduction. Then, we chose to deposit Cd and S from ammonia buffer and Se from acetic buffer, so as to shift Se reduction toward less negative potentials. The electrochemical behavior of Se(IV) in acetic buffer is shown in Figure 1b that reports the progressive evolution of cyclic voltammograms as obtained by a continuous scan from −0.1 to −0.95 V on Ag(111). The broad peak at −0.25 is connected to the redissolution of Ag_2Se that is chemically formed when the silver electrode is immersed in the solution.[28,30] Due to the faster kinetics in acidic media, the reduction peak of Se(0) to Se(−II) is already observed in the first scan. The peak decreases in the successive scans, thus indicating the progressive consumption of Se(IV). In fact, if fresh Se(IV) solution is introduced in the cell, the peak increases again. A further difference with

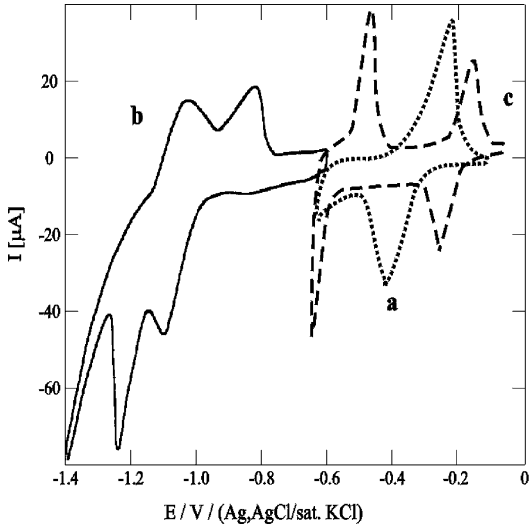

Figure 2. Cyclic voltammograms for CdS ECALE deposition: reductive UPD of Cd on a Se-covered Ag(111) from 1 mM $CdSO_4$, as recorded from −0.15 V (a); oxidative UPD of S recorded from −1.4 V on a previously deposited Cd layer (b); reductive UPD of Cd recorded from −0.1 V on a previously deposited S layer (c). All curves were recorded in pH 8.5 ammonia buffer solutions. The scan rate was 50 mV s^{-1}.

the cyclic voltammograms obtained in ammonia buffer is given by the absence of the reoxidation peak. On the contrary, during the reverse scan, the current is still cathodic, thus indicating the predominance of a reduction process.

The experimental conditions for the attainment of Se_{UPD} layers were deduced from Figure 1b: bulk Se(0) was obtained from 0.5 mM Se(IV) solutions by applying a potential $E = -0.7$ V for 2 s, then changing the Se(IV) solution with acetic buffer alone, shifting the potential to −0.8 V and waiting 45 s at this potential to reduce the excess of bulk Se(0). Finally, the cell was again washed with acetic buffer to eliminate the products of Se(0) reduction.

Procedure of ECALE Deposition of CdS_xSe_{1-x}. In analogy to the procedures used for the attainment of the ternary $Cd_xZn_{1-x}X$ (X = S, Se), the ECALE procedure to obtain CdS_xSe_{1-x} consists of alternating CdSe and CdS depositions.

To obtain CdSe, Cd was deposited at underpotential on the previously deposited Se.[29] Curve a in Figure 2 shows the reductive underpotential deposition of Cd on a Se-covered Ag(111) substrate from a 1 mM Cd(II) solution in pH 9.6 ammonia buffer. The Cd_{UPD} layer was obtained by applying a potential $E = -0.5$ V for 60 s. After Cd deposition, the cell was rinsed with ammonia buffer.

The ECALE cycle for the ternary compound growth was then completed by depositing CdS. Curve b in Figure 2 shows the oxidative underpotential deposition of S from 0.5 mM sulfur solutions on a Cd layer. Here, the unambiguous assignment of each peak would require more detailed investigation. However, for the purposes of this paper, it is sufficient to note that S UPD on Cd takes place at more negative potentials than on Ag(111).[13] This behavior is consistent with a more negative free energy change involved in the formation of CdS (−156.5 kJ mol^{-1}) than in that of Ag_2S (−40.7 kJ mol^{-1}). The S_{UPD} layer was obtained by applying a potential $E = -0.68$ V for 60 s. After S deposition, the cell was rinsed again with ammonia buffer.

Finally, curve c in Figure 2 shows the reductive underpotential deposition of Cd from 1 mM Cd(II) solutions

(29) Loglio, F.; Innocenti, M.; D'Acapito, F.; Felici, R.; Pezzatini, G.; Salvietti, E.; Foresti, M. L. *J. Electroanal. Chem.* **2005**, *575*, 161−167.
(30) Kazacos, M. S.; Miller, B. *J. Electrochem. Soc.* **1980**, *127*, 869.

on a S layer. A well-defined UPD peak is observed at approximately −0.3 V, whereas the beginning of a second UPD peak is observed at −0.6 V. The second UPD peak cannot be completely recorded since it overlaps bulk Cd deposition and it can never be isolated from bulk Cd deposition. However, it can be evidenced by keeping the electrode at −0.65 V to accumulate Cd on the electrode, and by then anodically stripping the deposit. The oxidative stripping peaks of Cd recorded after keeping the electrode at −0.65 V for 30, 60, and 120 s have a constant height. On the contrary, the first UPD peak can be easily separated by keeping the electrode at −0.5 V. Note that Cd UPD on S takes place at potentials less negative than on Se. In fact, due to the more negative free energy of formation of CdS, Cd UPD on S is more anticipated with respect to bulk deposition than on Se. As already stated, the basic ECALE cycle corresponds to the alternated deposition of CdSe and CdS that can be repeated as many times as desired to obtain deposits of practical importance.

However, this 1:1 sequence did not yield the expected stoichiometry with 50% of S and 50% of Se. On the contrary, XPS analysis revealed the expected 1:1 stoichiometric ratio between Cd and the anions, but a very high percentage of Se, corresponding to the compound $CdS_{0.2}Se_{0.8}$. According to the procedures adopted for the other ternary compounds obtained by ECALE,[10] the most effective way to increase the amount of S in the deposit consists of depositing more CdS cycles per CdSe cycle. These findings indicate that the presence of Se hinders S deposition; as an example, the compound with 50% S and 50% Se is obtained by performing two deposition cycles of CdSe for every five deposition cycles of CdS. This corresponds to the following sequence: Se/Cd/ Se/Cd/S/ Cd/S/Cd/S/Cd/S/Cd/S/Cd....

XPS Investigations of the Stoichiometry of CdS_xSe_{1-x}. The stoichiometry of the compounds obtained with different deposition sequences was determined by ex situ X-ray photoelectron spectroscopy (XPS) in ultrahigh vacuum. The right 1:1 ratio between cations and anions was found for all compounds examined, whichever was the stoichiometry. It must be noted that XPS measurements also yield the oxidation state of the single elements, and, indeed, the formation of the ternary compounds was confirmed: Cd is present as a cation, Cd(II), and S/Se as a anion, e.g., S(−II).

The stoichiometry of the compounds depends on the deposition sequence with a well-defined and reproducible trend (Figure 3). All measurements were carried out on samples formed with 100 deposition cycles of Cd and 100 deposition cycles of (S or Se) but with different CdSe/CdS deposition sequences. As already stated, the amount of S in the deposit increases while increasing the number of CdS cycles per CdSe cycle.

Systematic Investigation of the Ternary Sulfide Obtained with Different Deposition Sequences.

An additional characterization was performed in situ by electrochemical techniques. In practice, the deposited compounds are dissolved by the electrochemical stripping.

To this end, the potential is shifted toward positive potentials to force Cd dissolution. After all the Cd has been removed, the remaining chalcogen atoms are stripped by scanning the potentials toward negative values. This procedure is applied to the deposits obtained with CdSe/CdS deposition sequences (a) 1:1 and (b) 2:3.

(a) Deposition Sequence CdSe/CdS = 1:1. According to XPS measurements, this deposition sequence yields the compound $CdS_{0.2}Se_{0.8}$.

The amount of the elements deposited in a given number of cycles is estimated from the charge involved in the anodic stripping of the cation followed by the cathodic stripping of the anion. The potential of the stripping peak of Cd become progressively more positive as the number of deposition cycles increases. This behavior is shown by all compounds grown by ECALE.

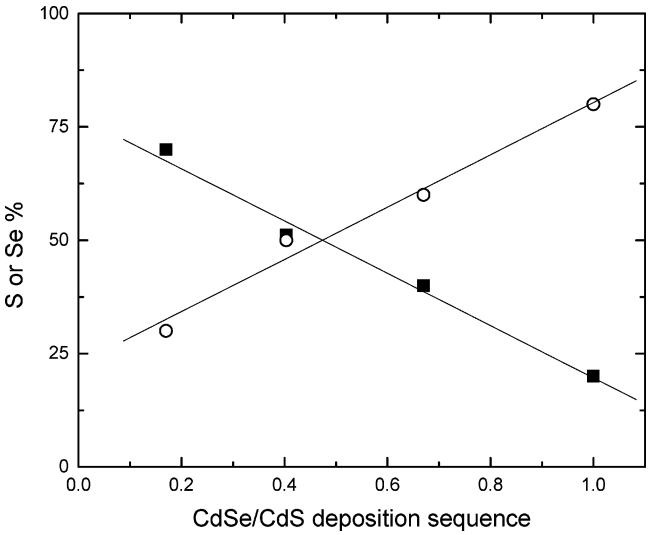

Figure 3. Plot of S (■) and Se (○) percentages as a function of the CdSe/CdS deposition sequences. All measurements were carried out on samples formed with 100 deposition cycles of (Se + S) and 100 deposition cycles of Cd.

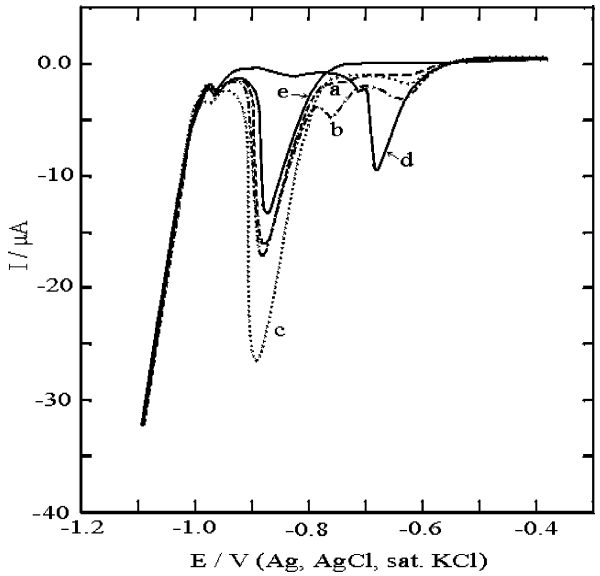

Figure 4. Stripping curves of the chalcogen atoms remained after Cd stripping for the deposition sequence CdSe/CdS = 1:1. For the sake of clarity, the figure is limited to the deposits obtained with the sequences Se/Cd/S/Cd/Se (a), Se/Cd/S/Cd/Se/Cd/S (b), and Se/Cd/S/Cd/Se/Cd/S/Cd/Se (c). The figure also reports the sequences Se/Cd/S (d) and Se/Cd/Se (e), which do not yield the ternary compound but are used for the unambiguous identification of Se and S stripping peaks. The scan rate was 10 mV s^{-1}.

It is interesting to analyze the stripping curves of the chalcogen atoms remained after Cd stripping. For the sake of clarity, Figure 4 is limited to the deposits obtained with the following sequences:

Se/Cd/S/Cd/Se curve a

Se/Cd/S/Cd/Se/Cd/S curve b

Se/Cd/S/Cd/Se/Cd/S/Cd/Se curve c

Figure 4 also reports the sequences Se/Cd/S (curve d) and Se/Cd/Se (curve e), which do not yield the ternary

compound, but are used for the unambiguous identification of Se and S stripping peaks.

The tiny peak at $E = -0.97$ V observed in all curves corresponds to the UPD layer of Se on Ag(111). This layer is more bound to the substrate, and therefore, it is reduced at more negative potentials than the bulk Se deposits. Except for a small bump at −0.62 V, curves a and c exhibit a predominant peak at the potential of Se stripping. This means that when it is deposited in the ternary compound, most of S is redissolved together with Se. The small bump at −0.62 V is probably ascribable to the dissolution of a limited amount of S. This amount is higher for the deposit that ends with S (curve b), probably since more S can be released from the top layer. As a matter of fact, curve b even shows two distinct peaks preceding the large peak at the potential of Se.

It must be noted that XPS results confirmed the presence of S, excluding the possibility that the attainment of a single stripping peak could be due to the unsuccessful deposition of S, or to some S removal.

As for all binary and ternary compounds already studied in our laboratory, the charge obtained by integrating the stripping peaks of films prepared with different number of deposition cycles gives the amount of the elements deposited for that number of cycles. The charge involved in the stripping increases linearly with the number of deposition cycles. Moreover, the charge involved in stripping the cations equals the charge involved in stripping the anions, thus indicating the right 1:1 stoichiometric ratio between Cd and (S + Se).

(b) Deposition Sequence CdSe/CdS = 2:3. According to XPS measurements, this deposition sequence yields the compound $CdS_{0.4}Se_{0.6}$.

The deposits were analyzed with the same criteria used for the sequence 1:1. Again, the charges involved in both metal and chalcogens strippings increase linearly with the number of ECALE cycles and have the same slope, indicating the 1:1 stoichiometric ratio.

Parts a and b of Figure 5 show the stripping peaks of S + Se following the stripping of Cd. Numbers on each curve indicate the number of Cd deposition cycles and, implicitly, the number of (Se + S) deposition cycles. Here, considering the higher percentage of sulfur of the compounds obtained with this deposition sequence, we distinguished between the deposits ending with S (Figure 5a) and those ending with Se (Figure 5b). With the only exception of curve 5 in Figure 5a, where the charge involved at potential of S stripping indicates that all S is reduced separately from Se, all other curves show that most of S is reduced together with Se. In addition, the samples ending with S yield a higher stripping peak at the potentials of S. However, the charge involved in this peak progressively decreases, indicating that, as for the sequence 1:1, only the outer S layers are redissolved in the region typical of S, whereas the inner layers are stripped together with Se. On the contrary, no significant differences were observed in the stripping curves of the metal.

As for the CdSe/CdS = 1:1 deposition sequence, the charge involved in the stripping increases linearly with the number of deposition cycles, and the charge involved in stripping the metal equals the charge involved in stripping the chalcogen atoms, indicating the right 1:1 stoichiometric ratio between Cd and (S + Se). These results are consistent with a layer by layer growth mechanism.

Morphological Characterization. Ex situ AFM measurements were performed to study the morphology for various stoichiometries of the ternary sulfoselenides.

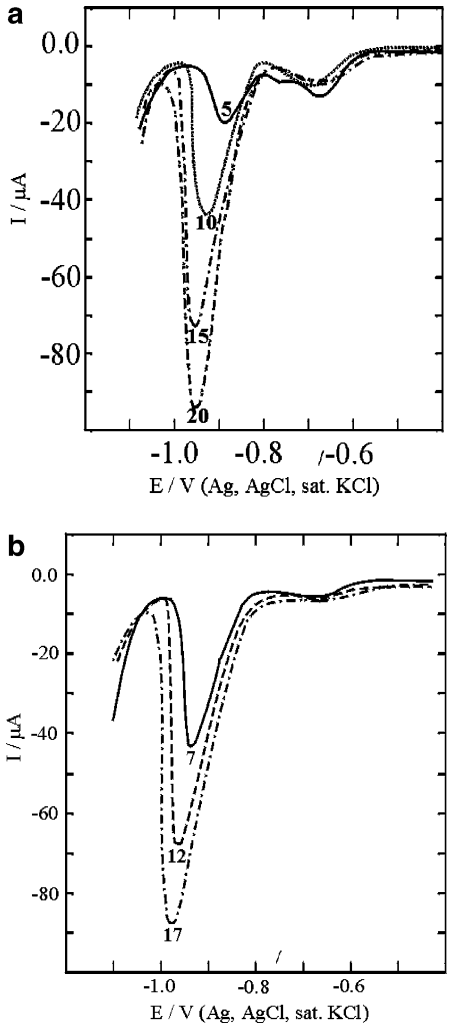

Figure 5. Stripping curves of the chalcogen atoms remained after Cd stripping for the deposition sequence CdSe/CdS = 2:3 for deposits obtained with sequences ending with S (a) and Se (b). Numbers on each curve indicate the number of (Se + S) ECALE cycles. The scan rate was 10 mV s^{-1}.

Figure 6 shows 5 × 5 μm^2 AFM images of CdS_xSe_{1-x} with different x values but obtained with the same 100 deposition cycles. The sampling resolution was 512 × 512. All images show the presence of a three-dimensional growth contribution. The figure also shows a well-defined trend of the roughness and of the cluster's size: qualitatively, both appear to decrease for larger x values.

The sample quality was checked through the root-mean-square roughness parameter (RMS) provided by the AFM software. RMS roughness was calculated via the standard formula:[31,32]

$$R_q = \sqrt{\frac{\sum_{k=1}^{M-1}\sum_{l=1}^{N-1}(Z_{k,l} - \bar{Z})^2}{MN}} \qquad (2)$$

with

$$\bar{Z} = \frac{1}{MN}\sum_{k=0}^{M-1}\sum_{l=0}^{N-1} Z_{k,l}$$

Here, $Z_{k,l}$ is the height of pixel kl; $\bar{Z}$ is the mean value of distribution; and $M \times N$ is the number of pixels, and, therefore, of data points.

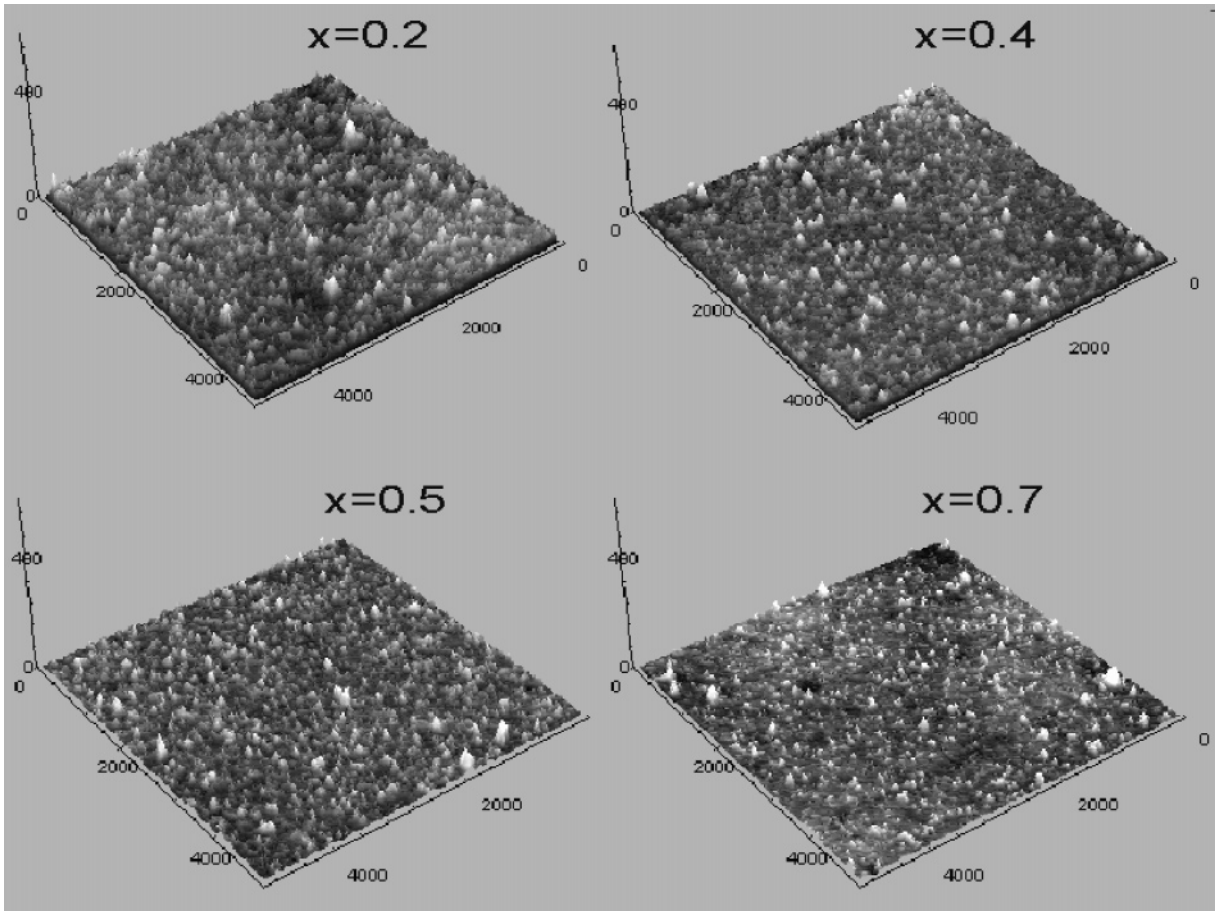

Figure 6. $5 \times 5\ \mu m^2$ AFM images of CdS_xSe_{1-x} with different x values but obtained with the same 100 deposition cycles. The sampling resolution was 512×512. $5 \times 5\ \mu m^2$.

The morphological analysis performed on samples of different stoichiometry obtained with 100 deposition cycles showed a marked decrease of roughness (from 14 nm for $CdS_{0.2}Se_{0.8}$ to 7 nm for $CdS_{0.7}Se_{0.3}$) while increasing the S percentage in the compound. The comparison with the cluster's diameter indicates that the low roughness value is partially ascribable to a progressive packing of the deposit due to the concomitant decrease of the cluster's diameter (from 110 nm for $CdS_{0.2}Se_{0.8}$ to 85 nm for $CdS_{0.7}Se_{0.3}$).

It must be stressed that, in principle, the presence of both 2D and 3D growth mechanisms does not exclude epitaxy. However, the presence of three-dimensional contributions deserves a thorough comment. The growth mechanism of thin layer compounds through the alternate underpotential deposition of the elements that form the compound can be only partially depicted by applying the concepts of metal electrocrystallization (discussed, e.g., in ref 33). The most important parameters determining the mechanism of UPD and OPD of a metal, Me, on a foreign substrate, S, are the Me_{ads}−S binding energy and the crystallographic misfit between S and a 3D Me bulk deposit. Accordingly, a 2D Me_{ads} phase is formed in the UPD range whereas a 3D Me_{ads} phase is formed in the OPD range. More specifically, one or more 2D Me_{ads} monolayers are formed when the binding energy of Me_{ads} on the foreign substrate is higher than that on native substrate Me; afterward, the growth can proceed according to two different mechanisms: the Frank-van der Merwe, FM, or the Stranski−Krastanov, SK, growth mode. The FM mode represents the layer-by-layer growth that occurs in systems with negligible crystallographic Me−S misfit, whereas the SK mode describes the formation of unstrained 3D Me island on top of strained 2D Me_{ads} on S. However, a three-dimensional contribution cannot be excluded even in the UPD range. This is what actually occurs in Me UPD systems with nonvanishing solubility of Me in S, where the formation of a 2D Me−S surface alloy and/or a 3D Me−S bulk alloy becomes energetically possible even in the UPD range. This could be one of the reasons for the 3D contribution observed in our case, since mixing two elements that form a compound is not much different from mixing two metals that form an alloy. In addition, STM studies carried out on both S[34] and Se[35] deposited at underpotential on Ag(111), as well as on the layer of Cd deposited at underpotential on S-covered Ag(111)[34] revealed very strained structures. On the contrary, XPD.[36] measurements carried out on thicker deposits of CdS deposited by ECALE revealed that the compound grows along the basal plane of wurtzite with a well-defined relation with the Ag(111) substrate, thus indicating that the strain of the first layer disappeared. This behavior could suggest a growth mode similar to the SK. Of course, the analogy is limited by the fact that we

(31) In *Reference guide of the Scanning Probe Image Processor (SPIP)*.
(32) Kiely, J. D.; Bonnell, D. A. *J. Vac. Sci. Technol. B* **1997**, *15* (4), 1483−1493.
(33) Budevski, E., Staikov, G., Lorenz, W. J. *Electrochemical Phase Formation and Growth*; VCH: Weinheim, Germany, 1996.
(34) Foresti, M. L.; Pezzatini, G.; Cavallini, M.; Aloisi, G.; Innocenti, M.; Guidelli, R. *J. Phys. Chem. B* **1998**, *102*, 7413.
(35) Cavallini, M.; Aloisi, G.; Guidelli, R. *Langmuir* **1999**, *15*, 2993.
(36) Cecconi, T.; Atrei, A.; Bardi, U.; Forni, F.; Innocenti, M.; Loglio, F.; Foresti, M. L.; Rovida, G. *J. Electron Spectrosc. Relat. Phenom.*, **2001**, *114−116*, 563.

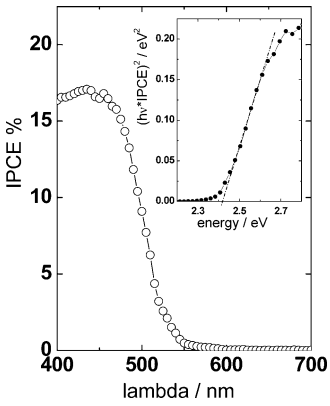

Figure 7. Photocurrent action spectrum of a CdS layer deposited on Ag, recorded at $E = -0.88$ V. Electrolyte: 1 M NaOH, 1 M Na_2S. Inset: direct transition plot with intercept showing the band gap energy ($E_g \cong 2.42$ eV).

operate in the UPD range, whereas OPD range is needed to grow bulk metal on the first upd layers. These circumstances, together with the unavoidable presence of defects in the real silver single crystals used as substrates are the probable reasons for the limited three-dimensional contribution that has already been observed for other compounds grown by ECALE.[11] In the case of CdS_xSe_{1-x}, the three-dimensional contribution is perhaps more important, due to the OPD step of the procedure adopted for Se_{UPD} layer formation.

Photoelectrochemical Characterization. The measurements were performed in a polysulfide solution (1 M NaOH, 1 M Na_2S and 50 mM S) of the type used to stabilize CdX photoanodes (X = S, Se; see refs 37−41). All materials showed negative photopotentials at open circuit and anodic photocurrents, as typical of n-type semiconductors. The dark open circuit potential of a Pt electrode in this medium is E ≅ − 0.78 V; the potential of CdX film electrodes (E = −0.85/−0.90 V) is close to that of the Ag/Ag_2S redox couple ($E° = -0.71\ V_{nhe}$[42]), suggesting control by corrosion phenomena occurring at the Ag surface exposed to the electrolyte, in correspondence of film imperfections.

Let us consider first CdS electrodes. Given the flatband position estimated in the literature (reported values are rather scattered in the range −1.75 to −1.20 V vs SCE in alkaline polysulfide[38−41]), at the potential of measurement ($E = -0.88$ V) the material is polarized under depletion. Figure 7 shows the spectral dependence of IPCE, the incident-photon-to-photocurrent-conversion-efficiency defined as the ratio of the flux of photogenerated electrons in the external circuit to photon flux on the electrode. As discussed elsewhere,[43] on the basis of the material properties the space charge region should extend over the entire film thickness d, estimated for these films in 20−25 nm. In these conditions, the IPCE at a given wavelength may be estimated by simply applying the Beer−Lambert law (using the absorption coefficient, e.g., $\alpha = 8 \times 10^6\ m^{-1}$ for $\lambda = 450$ nm, see ref 44). Comparing the experimental photocurrent values with the calculated ones, quantum efficiencies of photoconversion (per absorbed photon) are estimated to be a large fraction of 1.[43]

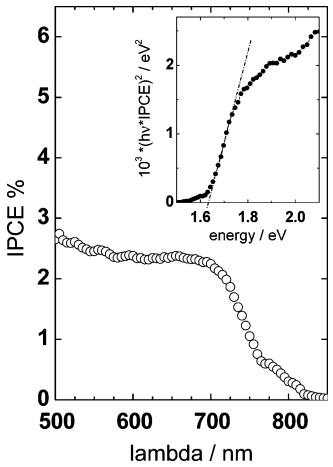

Figure 8. Photocurrent action spectrum of a CdSe layer deposited on Ag, recorded at $E = -0.88$ V. Electrolyte: 1 M NaOH, 1 M Na_2S. Inset: direct transition plot with intercept showing band gap energy ($E_g \cong 1.64$ eV).

The inset reported in Figure 7 shows a plot according to the relation

$$(\mathrm{IPCE}^* h\nu)^2 \propto (h\nu - E_g) \qquad (3)$$

valid for direct optical transitions;[45] the linear portion of the plot may be extrapolated to $E_g = 2.42$ eV, exactly the band gap of single-crystal CdS.[46,47] Hence, CdS films prepared by ECALE have properties close to those of single crystalline material, and show superior quality in comparison with materials obtained by other wet techniques[44,48,49] which cannot warrant the same control of structure and composition.

Figure 8 shows the photocurrent spectrum of CdSe. Considering the flatband values reported in the literature, $E_{FB} \cong -1.4\ V_{SCE}$[50,51]), at the measurement potential of $-0.88\ V_{SCE}$, CdSe is polarized under depletion. The IPCE values are markedly lower than those obtained for CdS, and the quantum efficiency per absorbed photon estimated on the basis of the Beer−Lambert law (using $\alpha = 3 \times 10^6\ m^{-1}$ for $\lambda = 700$ nm; see ref 50) is also lower, typically not exceeding 0.1−0.2. The direct transition plot[45] reported in the inset of Figure 8 gives an estimated band gap energy $E_g = 1.64$ eV, significantly below literature values (1.7−1.74 eV; see[13,14,51−53]). A similar value has been reported for Se rich $CdSe_{1+x}$ films, and the subband gap response was attributed to band tail states associated with defects.[53] Spectra of films deposited from acetic buffer and ammonium buffer show similar photocurrent intensities and the same E_g.

(37) Ellis, A. B.; Kaiser, S. W.; Wrighton, M. S. *J. Am. Chem. Soc.* **1976**, *98*, 1635.
(38) Meissner, D.; Memming, R.; Kastening, B. *J. Phys. Chem.* **1988**, *92*, 3476.
(39) Ellis, A. B.; Kaiser, S. W.; Bolts, J. M.; Wrighton, M. S. *J. Am. Chem. Soc.* **1977**, *99*, 2839.
(40) Richardson, J. H.; Perone, S. P.; Deutscher, S. B. *J. Phys. Chem.* **1981**, *85*, 341.
(41) Finlayson, M. F.; Wheeler, B. L.; Kakuta, N.; Park, K. H.; Bard, A. J.; Campion, A.; Fox, M. A.; Webber, S. E.; White, J. M. *J. Phys. Chem.* **1985**, *89*, 5676.
(42) Dobos, X. *Electrochemical Data*; Elsevier, Amsterdam, 1975.
(43) Innocenti, M.; Cattarin, S.; Cavallini, M.; Loglio, F.; Foresti, M. L. *J. Electroanal. Chem.* **2002**, *532*, 219.
(44) Peter, L. M. *Electrochim. Acta* **1978**, *23*, 1073.
(45) Butler, M. A. *J. Appl. Phys.* **1977**, *48*, 1914.
(46) Sze, S. M. *Physics of Semiconductor Devices*; 2nd ed.; Wiley: New York, 1981.
(47) Heller, K. C. Chang; Miller, B. *J. Electrochem. Soc.* **1977**, *124*, 697.
(48) Doña, J. M.; Herrero, J. *J. Electrochem. Soc.* **1992**, *139*, 2810.
(49) Doña, J. M.; Herrero, J. *J. Electrochem. Soc.* **1997**, *144*, 4091.
(50) Russak, M. A.; Reichman, J.; Witzke, H.; Deb, S. K.; Chen, S. N. *J. Electrochem. Soc.* **1980**, *127*, 725.
(51) Heller, A.; Schwartz, G. P.; Vadimsky, R. G.; Menezes, S.; Miller, B. *J. Electrochem. Soc.* **1978**, *125*, 1156.
(52) Noufi, R. N.; Kohl, P. A.; Rogers, J. W.; White, J. M.; Bard, A. J. *J. Electrochem. Soc.* **1979**, *126*, 949.
(53) Reichman, J.; Russak, M. A. *J. Electrochem. Soc.* **1981**, *128*, 2025.

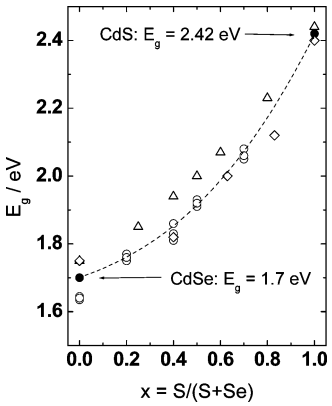

Figure 9. Band gap as a function of the composition parameter $x = S/(S + Se)$ for ECALE ternary compounds CdS_xSe_{1-x} (empty dots), compared with literature data: films prepared by vacuum evaporation[13] (empty diamonds); films prepared by spray pyrolysis[14] (empty triangles); bulk crystals[46,47] (full dots). The dashed curve is merely reported as a guide for the eye.

The spectra of ternary films of CdS_xSe_{1-x} measured at a potential of −0.88 V, show IPCE values comparable with those determined for CdSe, and the onset of photocurrent is again consistent with a direct transition. The dependence of band gap energy on the composition parameter x is shown in Figure 9: the band gap values estimated for ternary ECALE films are in good agreement with literature data for films prepared by vacuum evaporation[13] and spray pyrolysis.[14]

Conclusions

Cadmium sulfoselenides were grown on Ag (111) by the electrochemical atomic layer epitaxy (ECALE) method. Deposition of CdSe appeared to be favored with respect to CdS deposition: a deposition sequence 1:1 of the two binary species produces a ternary compound of composition $CdS_{0.2}Se_{0.8}$.

The charge involved in stripping either the metal or the chalcogen atoms from CdS_xSe_{1-x} increases linearly with the number of deposition cycles, thus supporting a layer-by-layer growth, at least concerning the first stages of the film formation. Moreover, regardless of the stoichiometry of the ternary compound obtained, the two charges are equal, thus confirming the right 1:1 stoichiometric ratio estimated from XPS data.

Morphology and electronic properties of the ternary compounds have been characterized as a function of the composition and compared with the corresponding binary compounds CdS and CdSe. Ex situ AFM measurements were performed to characterize the morphology on varying the stoichiometry of the ternary sulfoselenides. For all compounds examined, the morphological analysis indicates that a three-dimensional growth occurs in addition to the two-dimensional growth on increasing the film thickness. Moreover, the roughness decreases while increasing S percentage according to the concomitant decrease of the cluster's size which determines a better deposit packing.

Photoelectrochemical measurements on CdS show good efficiency of photoconversion and the band gap typical of the single crystal; conversely, photospectra recorded at CdSe show lower efficiency and the presence of subband gap response. Among the possible reasons, we mention some crystalline disorder originating from the two-steps deposition procedure of Se (massive deposition and stripping of the excess). However, the observed dependence of the band gap E_g on the composition parameter x for the ternary species CdS_xSe_{1-x} is monotonic and close to that reported in the literature, confirming formation of a single, essentially homogeneous phase.

As already stated, the presence of both 2D and 3D growth mechanisms does not necessarily exclude epitaxy.[33] Nevertheless, the concomitant presence of three-dimensional contributions and relatively small cluster's sizes seems to indicate significant deviations from ideal epitaxial growth and, therefore, some limits in the application of the ECALE method to deposition of cadmium sulfoselenides. However, the ECALE procedure maintains over traditional wet techniques the great advantage of an excellent control on composition.

Acknowledgment. The authors are grateful to Dr. Stefano Caporali for XPS measurements. They also thank Andrea Pozzi for technical assistance and Ferdinando Capolupo for the preparation of the silver single crystal electrodes. The financial support of the Murst and of the Consorzio Interuniversitario per la Scienza e Tecnologia (INSTM) is gratefully acknowledged.

LA050176K